URSI GASS 2021, Rome, Italy, 28 August - 4 September 2021

On the Impact of Rectifier Topologies on Rectennas performance

Kyriaki Niotaki
Télécom Paris, Palaiseau, France

Abstract

This work focuses on the impact of the rectifier topology selection on rectennas performance and especially on their RF-dc conversion efficiency. The performance of the main rectifier topologies over a range of input power and output load values is analyzed and the optimum operating conditions for each topology are identified. This work aims to help RF designers to identify and select the most appropriate topology based on their application needs.

1 Introduction

Wireless Sensor Networks (WSN) require a plethora of interconnected devices to provide core facilities for smart cities and the Internet of Things (IoT) applications. According to [1], 40 billion IoT devices will be installed by 2025. Powering this large number of devices is extremely challenging. Sensor nodes cannot rely on batteries as their power source for a number of reasons, amongst which environmental impact. Disposing billions of batteries is not ecologically friendly while the maintenance cost due to the batteries replacement will be high [2]. To overcome these limitations associated with the long scale deployment of WSN, there has been a recent interest exploring the possibility of powering up the devices using Radio Frequency (RF) Energy Harvesting (EH) solutions or Wireless Power Transfer (WPT) technologies.

A typical sensor node powered by RF EH or WPT, in its simpler form, consists of an antenna and a rectifier (or rectenna for short) and the load (application). The RF energy is collected from the antenna that converts it to dc power using a certain rectifying element, such as Schottky diode(s). To ensure maximum power transfer of the received RF power, a matching network is placed between the antenna and the rectifying element. Various rectifier topologies have been presented in the literature, such as half-wave rectifier and n-stage Dickson rectifiers. The goal of this work is to identify the operating conditions under which each rectifier topology shows best performance.

The knowledge of the operating conditions, such as input power range and output load, is prerequisite for the selection of the optimum topology. Here, the impedance characteristics of the rectifier topologies are initially analyzed through simulations. Then, the performance of each rectifier topology over load and power variation is compared. Finally, the impact of the number of stages of the rectifier topologies on the system performance is presented.

2 Design Challenges

The most widely used metric for the performance of rectifiers is their RF-dc conversion efficiency. Each rectifier topology shows maximum RF-dc conversion efficiency for a fixed output load and input power level, while their performance degrades when deviating from the nominal operating conditions. To achieve maximum rectenna efficiency, one has to select the rectifier topology that will behave better under the expected operating conditions: input power level and output load.

The available RF power levels in the environment are typically low while the power variability over time and location make the rectifier design even more challenging. Figure 1 shows the measured peak RF power in various locations around the world [2]. Despite the low-power levels, the total power across a wireless channel is typically quite higher; the measured power 6.3 km far from a TV station in Tokyo was -35 dBm in [3], while the total power over 60 MHz bandwidth was - 9 dBm.

Similarly, the load varies at the rectifier output versus time. An example of a time varying load is presented in [4], where the load varies from around 100 Ohm to 600 kOhm for different states of operation. The aforementioned varying operating conditions of the rectifier result in a variation of its impedance characteristics and thus a degraded performance [5]. To demonstrate the impact of the input power and output load variations on the rectifiers performance, the rectifier equivalent circuitry is analyzed here.

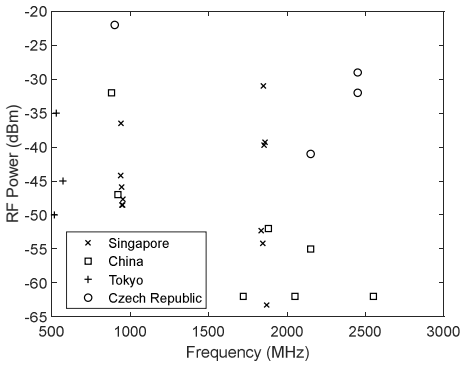

Figure 1. Measured environmental power level at various locations worldwide.

The behavior of a half-wave rectifier, single-stage and two-stage Dickson rectifier topology over power and load variations (Figure 2(a)-(c)) is analyzed here. The equivalent network of each rectifier consists of combination of a shunt resistor R_e and a capacitive component C_e, as it is shown in Figure 2(d).

The rectifier topologies are optimized to operate at the sub-1 GHz range. The results are obtained through Harmonic Balance (HB) simulation in a commercial simulator (Advanced Design System). The SMS7630 diode model is used in the simulations and the antenna is represented as a 50 Ohm source.

Figure 3 presents a comparison of the equivalent R_eC_e network of the rectifiers and the ratios between the largest and smallest value of R_e and C_e are summarized in Table I. The variation of the equivalent R_e and C_e values are shown over an input power range of -30 dBm to 3 dBm and versus output load (from 5 Ohm to 100 kOhm).

One can notice that there is a larger range of variation of the equivalent resistance (R_e) for the half-way rectifier topology if compared with the other two topologies, which show similar behavior in terms of R_e variation. The larger R_e variation of the half-wave rectifier (174:1 ratio) implies that it is more difficult to match the diode to the antenna. In terms of C_e variation, the value of the equivalent capacitive component of the rectifier topology strongly depends on the rectifier topology and the number of diodes. However, in any case the capacitor varies in a similar manner.

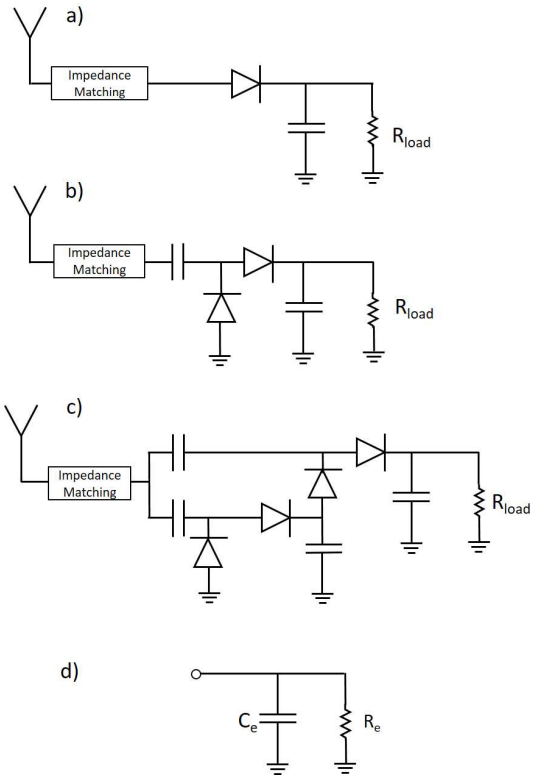

Figure 2. Main rectifier topologies: a) half-wave rectifier b) single-stage Dickson rectifier, c) two-stage Dickson rectifier and d) equivalent RC network of the rectifiers.

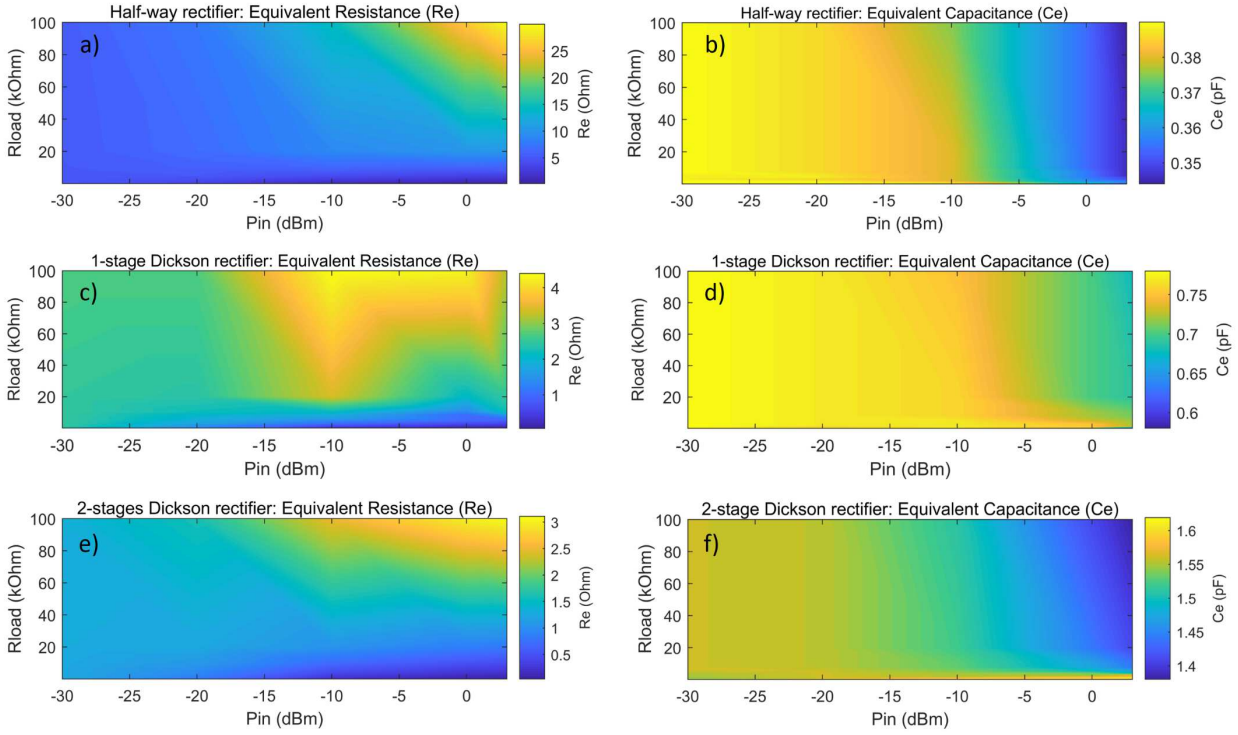

Figure 3. Equivalent $\boldsymbol{R_eC_e}$ network of the rectifiers: a) $\boldsymbol{R_e}$ and b) $\boldsymbol{C_e}$ for the half-way stage rectifier, c) $\boldsymbol{R_e}$ and d) $\boldsymbol{C_e}$ for the single-stage Dickson rectifier and e) $\boldsymbol{R_e}$ and f) $\boldsymbol{C_e}$ for the two-stage Dickson rectifier topology.

3 Performance Comparison

In order to evaluate the performance of the rectifier topologies under different operating conditions, the impedance matching network between the antenna and the rectifiers is designed and optimized at the sub-1 GHz frequency band. A simple matching network (series inductor and shunt capacitor) is used as the impedance matching network between the antenna and the diode(s) input(s), while the antenna is represented as a 50 Ohm source.

The rectifier topologies are optimized for maximum RF-dc conversion efficiency. The load which results at maximum RF-dc conversion efficiency for each topology is R_{load}=2 kOhm for the half-way rectifier and R_{load}=5 kOhm and R_{load}=10 kOhm for the single-stage and two-stage Dickson rectifier, respectively.

Similarly, the peak RF-dc conversion efficiency is achieved for P_{in}= -10 dBm for the half-way rectifier and P_{in}= -3 dBm and P_{in}= 0 dBm for the single-stage and two-stage Dickson rectifier topologies, respectively. The optimum operating conditions for each rectifier are summarized in Table II, while Table III presents the matching network components values for each topology.

Figure 4 shows the simulated RF-dc conversion efficiency of the rectifiers versus input power. One can notice here that the half-wave rectifier exhibits a peak RF-dc conversion efficiency at low power levels. In contrast, the peak efficiency of the n-stage Dickson rectifier topology is achieved for higher power levels; as the number of stages increases, the input power level for which the RF-dc conversion efficiency is maximum is increased as well.

TABLE **I**
EQUIVALENT R_e AND C_e

	R_e	C_e
Half-wave rectifier	0.17 - 30 Ohm (174:1 ratio)	0.34 - 0.39 pF (1.3:1 ratio)
Single-stage Dickson rectifier	0.06 - 44 Ohm (73:1 ratio)	0.58 - 0.78 pF (1.35:1 ratio)
Two-stage Dickson rectifier	0.04 to 3.1 Ohm (84:1 ratio)	1.38 to 1.6 pF (1.2:1 ratio)

TABLE **II**
OPTIMUM OPERATING CONDITIONS FOR EACH TOPOLOGY

	P_{in}	R_{load}
Half-wave rectifier	- 10 dBm	2 kOhm
Single-stage Dickson rectifier	- 3 dBm	5 kOhm
Two-stage Dickson rectifier	0 dBm	10 kOhm

Additionally, one can notice that the n-stage Dickson rectifier topology maintains its peak efficiency for a wider input power range levels and over a wider bandwidth.

Figure 5 presents the simulated RF-dc conversion efficiency versus output load variation. One can notice here that the optimum load strongly depends on the rectifier architecture and as the number of rectifier stages increases the optimum load value increases as well. Thus, it is important to identify the operating conditions of the rectifier in order to select the most appropriate topology and then optimize the rectifier performance accordingly. The design of the rectifier at non-realistic operating conditions will cause degradation of the rectifier performance and thus, reduce the harvested dc power.

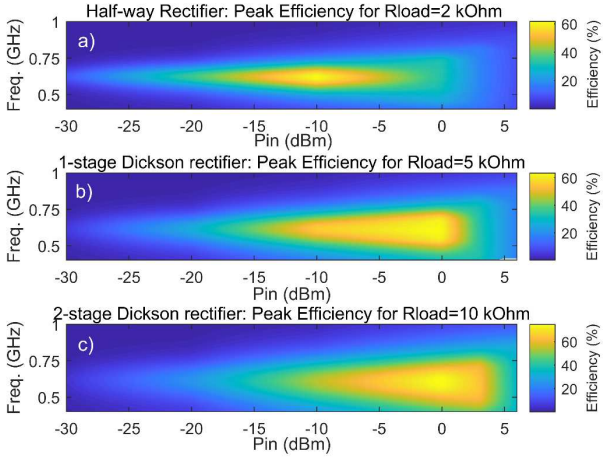

Figure 4. RF-dc conversion efficiency over frequency and input power variation for: (a) the half-way rectifier and R_{load} =2 kOhm, (b) the 1-stage Dickson rectifier and R_{load}=5 kOhm and (c) the 2-stage Dickson rectifier and R_{load}=10 kOhm.

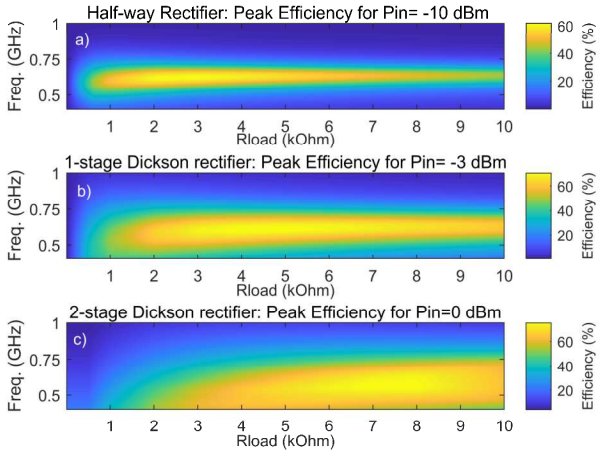

Figure 5. RF-dc conversion efficiency over frequency and output load variation for: a) the half-way rectifier and P_{in}= -10 dBm, b) the 1-stage Dickson rectifier and P_{in}= -3 dBm and c) the 2-stage Dickson rectifier and P_{in}= 0 dBm.

TABLE **III**
COMPONENTS VALUES USED FOR RESULTS IN FIG. 4- FIG. 5

	Series inductor	Shunt capacitor
Half-wave rectifier	L= 63.6 nH	C = 0.61 pF
Single-stage Dickson rectifier	L= 41.8 nH	C = 0.76 pF
Two-stage Dickson rectifier	L= 38 nH	C =0.1 pF

The obtained results are in agreement with the performance of state of the art rectifiers for energy harvesting applications. Figure 6 presents the optimum load for multi-band Dickson rectifier topologies operating at the sub-6 GHz frequency. Topologies with different diodes are considered. It can be observed that as the number of stages increases, the same applies for the optimum load value.

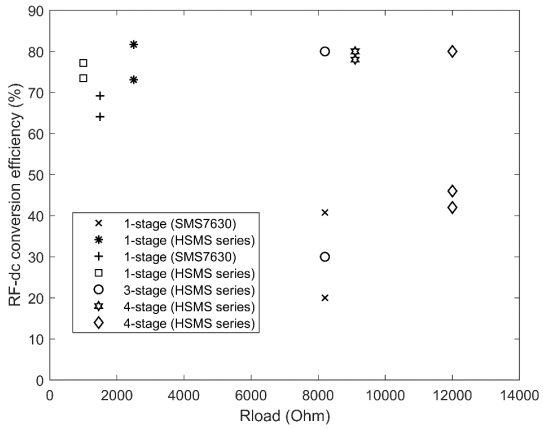

Figure 6. RF-dc conversion efficiency over optimum load values multi-stage rectifier topologies [6] - [12].

4 Conclusions

The performance of the main rectifier topologies for Energy Harvesting applications, over input power and output load variations, is analyzed and compared. The optimum operating conditions for each topology are identified. The obtained results can contribute to the selection of the most appropriate topology based on the application needs.

5 References

1. Eid, A., Hester, J.G.D. & Tentzeris, M.M. 5G as a wireless power grid. Sci Rep 11, 636 (2021), https://doi.org/10.1038/s41598-020-79500-x

2. J. Finnegan, K. Niotaki and S. Brown, "Exploring the Boundaries of Ambient RF Energy Harvesting with LoRaWAN," in IEEE Internet of Things Journal, doi: 10.1109/JIOT.2020.3030349.

3. R. J. Vyas, B. B. Cook, Y. Kawahara, and M. M. Tentzeris. E-WEHP: A Batteryless Embedded Sensor-Platform Wirelessly Powered From Ambient Digital-TV Signals. IEEE Transactions on Microwave Theory and Techniques, 61(6):2491–2505, Jun 2013 , doi: 10.1109/TMTT.2013.2258168.

4 C. Delgado, J. M. Sanz and J. Famaey, "On the Feasibility of Battery-Less LoRaWAN Communications Using Energy Harvesting," 2019 IEEE Global Communications Conference (GLOBECOM), Waikoloa, HI, USA, 2019, pp. 1-6, doi: 10.1109/GLOBECOM38437.2019.9013638.

5 J. Kimionis, A. Collado, M. M. Tentzeris and A. Georgiadis, "Octave and Decade Printed UWB Rectifiers Based on Nonuniform Transmission Lines for Energy Harvesting," in IEEE Transactions on Microwave Theory and Techniques, vol. 65, no. 11, pp. 4326-4334, Nov. 2017, doi: 10.1109/TMTT.2017.2697851.

6. D. Ho, I. Kharrat, V. Ngo, T. Vuong, Q. Nguyen and M. Le, "Dual-band rectenna for ambient RF energy harvesting at GSM 900 MHz and 1800 MHz," 2016 IEEE International Conference on Sustainable Energy Technologies (ICSET), Hanoi, 2016, pp. 306-310, doi: 10.1109/ICSET.2016.7811800.

7. J. Liu, M. Huang and Z. Du, "Design of Compact Dual-Band RF Rectifiers for Wireless Power Transfer and Energy Harvesting," in IEEE Access, vol. 8, pp. 184901-184908, 2020, doi: 10.1109/ACCESS.2020.3029603.

8. J. Liu, X. Y. Zhang and C. Yang, "Analysis and Design of Dual-Band Rectifier Using Novel Matching Network," in IEEE Transactions on Circuits and Systems II: Express Briefs, vol. 65, no. 4, pp. 431-435, April 2018, doi: 10.1109/TCSII.2017.2698464.

9. A. Jolly, M. Peer, V. A. Bohara and S. Verma, "Design and development of dual-band multi-stage RF energy harvesting circuit for low power applications," 2017 IEEE International Conference on Advanced Networks and Telecommunications Systems (ANTS), Bhubaneswar, 2017, pp. 1-5, doi: 10.1109/ANTS.2017.8384109.

10. Qiang Zhao et al., "Dual-band antenna and high efficiency rectifier for RF energy harvesting system," 2015 IEEE 6th International Symposium on Microwave, Antenna, Propagation, and EMC Technologies (MAPE), Shanghai, 2015, pp. 682-685, doi: 10.1109/MAPE.2015.7510410.

11. B. L. Pham and A. Pham, "Triple bands antenna and high efficiency rectifier design for RF energy harvesting at 900, 1900 and 2400 MHz," 2013 IEEE MTT-S International Microwave Symposium Digest (MTT), Seattle, WA, 2013, pp. 1-3, doi: 10.1109/MWSYM.2013.6697364.

12. H. M. Saraiva et al., "Experimental Characterization of Wearable Antennas and Circuits for RF Energy Harvesting in WBANs," 2014 IEEE 79th Vehicular Technology Conference (VTC Spring), Seoul, 2014, pp. 1-5, doi: 10.1109/VTCSpring.2014.7022920.